Chemical Geology 579 (2021) 120349

Contents lists available at ScienceDirect

Chemical Geology

journal homepage: www.elsevier.com/locate/chemgeo

Invited Research Article

Thallium behavior during high-pressure metamorphism in the Western Alps, Europe

Shelby T. Rader [a,b,*], Richard M. Gaschnig [b], Sean M. Newby [c], Gray E. Bebout [d], Michael J. Mirakian [b], Jeremy D. Owens [c]

[a] Department of Earth and Atmospheric Sciences, Indiana University, Bloomington, IN, United States of America
[b] Department of Environmental, Earth, and Atmospheric Sciences, University of Massachusetts Lowell, Lowell, MA, United States of America
[c] Department of Earth, Ocean, and Atmospheric Sciences, Florida State University, Tallahassee, FL, United States of America
[d] Department of Earth and Environmental Sciences, Lehigh University, Bethlehem, PA, United States of America

ARTICLE INFO

Editor: Catherine Chauvel

Keywords:
thallium
Schistes Lustrés
stable isotopes
subduction
Western Alps

ABSTRACT

Thallium (Tl) is a highly incompatible element which can be redistributed during various igneous and hydrothermal events such as mineral dehydration and low-temperature hydrothermal alteration. Despite the strong influence fluid-rock interactions can have on Tl redistribution and the importance of fluids in subduction-zone volatiles cycling, the geochemical behavior of Tl during high-P/T metamorphism has not yet been quantified. Here we provide new Tl isotope composition (ε^{205}Tl) and concentration ([Tl]) data for a suite of 18 metapelite and metacarbonate rocks from the Schistes Lustrés Complex and the nearby Lago di Cignana exposure in the western Alps. This suite represents metamorphism over a range of peak metamorphic *P-T* conditions of 300–550 °C and 1.5–3.0 GPa (similar to the range of *P-T* experienced in most modern subduction zones).

With increasing metamorphic grade, [Tl] shows no statistical variation while ε^{205}Tl initially remains fairly constant (in order of increasing grade, Fraiteve (unit A) $\varepsilon^{205}Tl_{avg} = -2.1$ ($\pm$ 0.3); Assietta (unit B) $\varepsilon^{205}Tl_{avg} = -1.6$ ($\pm$ 0.6); Albergian (unit C) $\varepsilon^{205}Tl_{avg} = -1.9$ ($\pm$ 0.5)) before shifting to more negative values during higher grade metamorphism (Finestre (unit D) $\varepsilon^{205}Tl_{avg} = -2.4$ ($\pm$ 0.3); Cignana (unit E) $\varepsilon^{205}Tl_{avg} = -3.5$ ($\pm$ 0.3)). Although it appears likely that Tl is largely retained in such rocks to depths approaching those of arc magma generation, the mineralogical hosts for Tl change during prograde devolatilization. This may contribute to a significant shift in ε^{205}Tl related to fractionation induced by only minor amounts of loss due to fluid-mineral partitioning. Prograde metamorphism results in the breakdown of chlorite and other minor mineralogical constituents, releasing chlorite-borne Tl that could be in part incorporated into phengite and in part lost to fluids. This study emphasizes the need for prograde mineral reaction history to be considered in studies of the retention or loss of trace elements such as Tl.

1. Introduction

Subduction is a fundamental process governing the mass transfer of Earth materials. Surface materials are transferred to the Earth's interior, where they can either be returned to the crust via arc magmatic processes or carried to great depth in the mantle. As such, subduction ultimately modifies the compositions of the major Earth reservoirs, including the oceans, lithosphere, and atmosphere (Korenaga, 2018; Spandler and Pirard, 2013; Taylor, 1977). However, significant questions remain regarding how efficiently trace elements are injected into the mantle as opposed to being recycled back to the surface via arc magamatism.

Several new, non-traditional stable isotope systems have recently been applied to subduction zone settings in an attempt to elucidate to what extent surface materials may be transferred to volcanic arcs (Barnes et al., 2019; Gaschnig et al., 2017; König et al., 2016; Prigent et al., 2018). One such system of particular interest, thallium (Tl), can be an indicator of sediment flux accompanying subduction (Nielsen et al., 2016) and shows differences in isotopic compositions in subducting material and resultant arc rocks in many locations (Blusztajn et al., 2018; Nielsen et al., 2017a; Prytulak et al., 2013). Shu et al. (2019) demonstrated that Tl isotope compositions can vary depending on the protolith as well as the metamorphic and metasomatic history of the

* Corresponding author.
E-mail address: shtrader@iu.edu (S.T. Rader).

https://doi.org/10.1016/j.chemgeo.2021.120349
Received 28 January 2021; Received in revised form 9 May 2021; Accepted 25 May 2021
Available online 27 May 2021

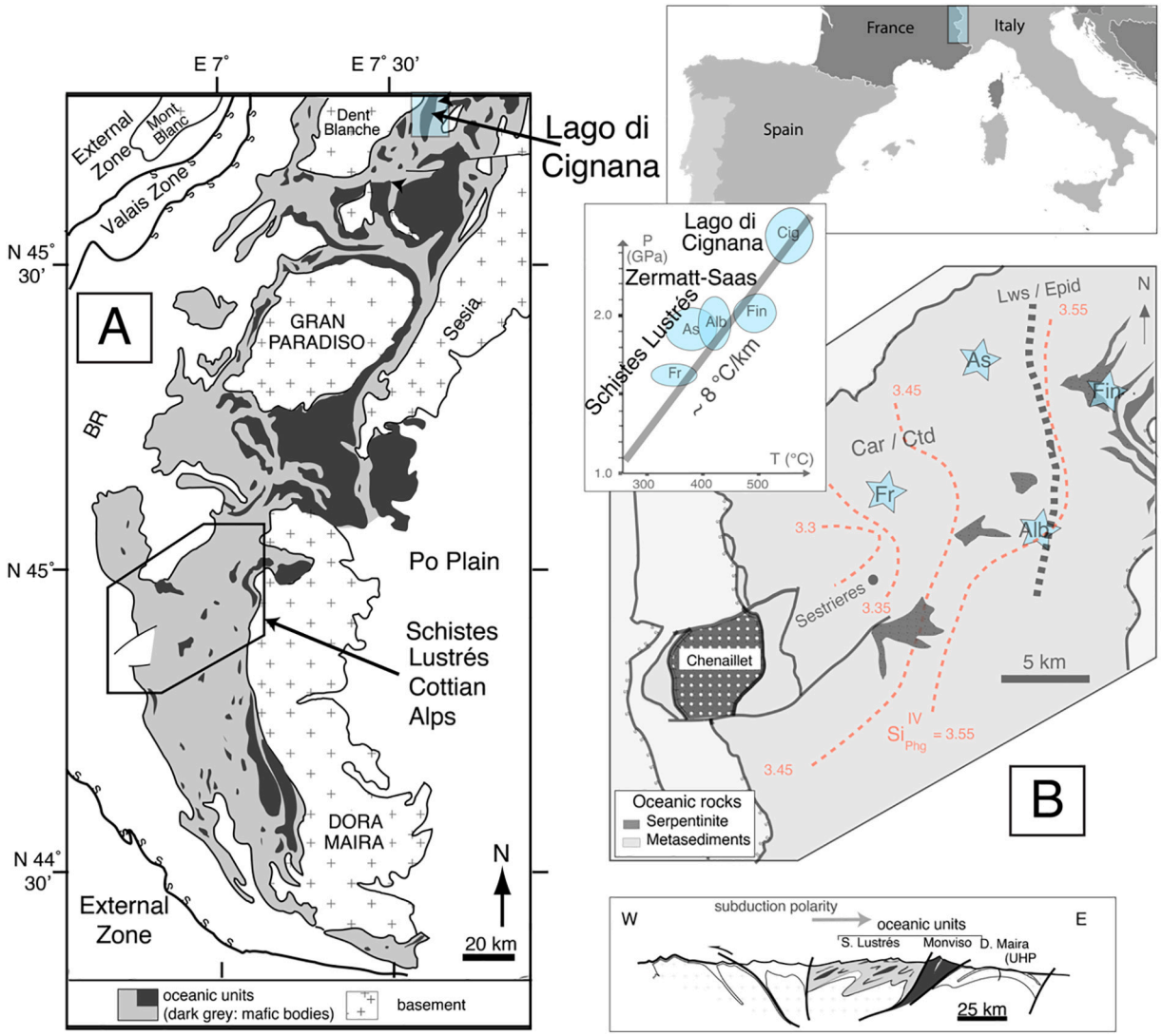

Fig. 1. Simplified geologic map of the Western Alps, showing the locations of Schistes Lustrés and Lago di Cignana samples (A.). Regional location of area is depicted, with Schistes Lustrés and Lago di Cignana regions highlighted in blue (B., upper panel). Schistes Lustrés sampling locations and traverse are enlarged for more detailed view (B.). Inset in B displays the pressure-temperature ranges for the peak metamorphic conditions for each subunit of the Schistes Lustrés (Fr = Fraiteve, As = Assietta, Alb = Albergian, Fin = Finestre) and Lago di Cignana (Cig). Figure is modified from Cook-Kollars et al. (2014) and *P-T* data are from Agard et al. (2001) and Angiboust et al. (2009). For coordinates of sampling locations, please refer to the Supplementary material.

sample For example, the incorporation of altered oceanic crust (AOC) can strongly influence the arc rock Tl isotope composition, and may even overwhelm other contributors to the Tl budget. Likewise, overprinting of the subducting materials by metamorphic fluids rich in Tl can result in arc rock Tl isotope compositions that are indistinguishable from mantle values. Additionally, the incorporation of Mn-rich pelagic sediments can shift arc rock Tl isotope compositions well outside the range of average mantle values as Mn oxides have a significant positive isotope signature (Nielsen et al., 2016). In fact, several redox-sensitive elements beyond Tl have exhibited an "isotopic mismatch" between subducted slab material and resultant arc magmas for some localities. This observed 'mismatch' has been attributed primarily to two potential sources: (1) the incorporation of an isotopically distinct sedimentary flux, and/or (2) the isotopic fractionation of redox-sensitive elements during slab dehydration, resulting in an isotopically unique 'fluid' (Andersen et al., 2015; Freymuth et al., 2015; Gaschnig et al., 2017; König et al., 2016; Prytulak et al., 2013).

Thallium has two redox states (Tl^{+} and Tl^{+3}), which have been invoked to explain the large variation in its isotope composition observed in a variety of geologic settings (Nielsen et al., 2017b). Variations in isotope composition are reported in epsilon units relative to the NIST 997 Tl standard in parts per 10,000:

$$\varepsilon^{205}Tl = \left({}^{205}Tl/{}^{203}Tl_{sample} - {}^{205}Tl/{}^{203}Tl_{NIST997}\right)/\left({}^{205}Tl/{}^{203}Tl_{NIST997}\right) \times 10,000$$

Adsorption and resultant uptake of oxidized Tl by pelagic clays and Fe/Mn oxides has produced the heaviest $\varepsilon^{205}Tl$ values currently observed on Earth (Nielsen et al., 2017a, 2017b; Rehkämper et al., 2004), with $\varepsilon^{205}Tl$ up to $\approx +15$. Conversely, the remobilization and deposition of reduced Tl during hydrothermal alteration of oceanic crust shifts $\varepsilon^{205}Tl$ compositions to much lower values ($\varepsilon^{205}Tl$ down to ≈ -15), particularly when compared with average mantle values ($\varepsilon^{205}Tl_{MORB/DMM} \approx -2$) (Nielsen et al., 2017a, 2017b; Rehkämper et al., 2004), or seawater values ($\varepsilon^{205}Tl \approx -6$) (Owens et al., 2017). Given that redox processes and interaction with various fluids can alter Tl isotope compositions to such extremes, it is increasingly pertinent to quantify the effects of fluid formation on the elemental and isotopic behavior of Tl in subduction processes, particularly as Tl is being used as a tracer of deep mantle recycling (Blusztajn et al., 2018; Nielsen et al., 2006; Prytulak et al., 2013; Shu et al., 2019).

Variably carbonate-rich metapelitic rocks of the Schistes Lustrés,

Table 1
Whole rock data for select elemental concentrations and thallium isotope compositions. Thallium data were collected in-house, all other major and trace element data are sourced from Epstein et al., 2020.

MM grade	Sample	Q-ICP-MS [Tl] (ng/g)	MC-ICP-MS [Tl] (ng/g)	ε^{205}Tl	2 σ	n	K_2O (wt%)	Rb (μg/g)	Cs (μg/g)	Cu (μg/g)	Fe_2O_3(T) (wt%)	MnO (wt%)
Fraiteve – grade A	SL98-2PELA	1119	613	−1.1	0.3	3	3.5	148	8.1	76	7.4	0.23
	SL99-19A	903	972	−2.2	0.1	3	3.1	170	10.5	100	6.8	0.11
	SL99-28A	1479	1524	−2.4	0.2	3	5.1	244	14.9	120	6.4	0.09
	SL99-30B	512	533	−2.8	0.4	3	1.9	88	5.2	50	8.4	0.81
	Average	*1003*	*910*	*−2.1*	*1.3*		*3.4*	*163*	*9.7*	*87*	*7.2*	*0.31*
Assietta – grade B	SL98-3PELD	1050	1154	−1.9	0.6	3	4.2	222	12.3	180	15.1	0.44
	SL99-37C	1124	1013	0.0	0.8	3	4.0	219	10.9	20	7.8	0.09
	SL99-38B	550	473	−2.1	0.9	3	1.3	76	4.5	60	3.7	0.22
	SL99-40C	635	733	−2.0	0.1	3	2.0	109	6.1	50	5.1	0.08
	Average	*840*	*843*	*−1.5*	*1.7*		*2.8*	*157*	*8.5*	*28*	*7.9*	*0.83*
Albergian – grade C	SL99-13A	343	402	−2.3	0.5	3	1.1	49	3.6	30	3.6	0.13
	SL99-16A	909	781	−1.5	0.4	3	4.7	185	9.2	70	8.0	0.07
	Average	*626*	*592*	*−1.9*	*0.8*		*2.9*	*117*	*6.4*	*50*	*5.8*	*0.10*
Finestre – grade D	PEL-962	437	452	−2.9	0.5	3	2.3		3	80	7.0	0.56
	SL99-34C	888	1033	−2.7	0.1	3	3.9	160	9.2	60	6.7	0.14
	SL99-41D	1612	1352	−1.7	0.2	3	5.5	250	12.5	60	6.8	0.08
	Average	*979*	*946*	*−2.4*	*1.0*		*3.9*	*205*	*8.2*	*67*	*6.8*	*0.26*
Cignana – grade E	02-LDCS-10	1020	1078	−3.3	0.5	3	3.4	158	7.8	50	7.0	0.86
	02-LDCS-11	1302	1505	−3.0	0.6	3	4.3	197	10.1	60	8.2	0.43
	LC99-4A	881	957	−3.8	0.3	3	2.9	127	6.3	100	5.6	0.23
	LC99-5A	519	603	−3.7	0.1	3	1.7	67	3.7	<10	3.4	0.99
	Average	*930*	*1036*	*−3.5*	*0.6*		*3.1*	*137*	*7.0*	*70*	*6.0*	*0.63*
BHVO-2	This study		21.9	−1.4	0.3	4						
	Published (Brett et al., 2018)		*23*	*−1.2*	*0.7*							
BCR-2	This study		316	−2.2	0.3	6						
	Published (Brett et al., 2018)		*306*	*−2.4*	*0.2*							
Nod-A-1	This study		120,500	11.2	0.3	3						
	Published (Nielsen et al., 2017a, 2017b)		*108,000*	*10.7*	*0.5*							

exposed in the Cottian Alps, Italy, provide an opportunity to examine the effects of prograde slab devolatilization on Tl concentrations, mineral residency, and isotopic composition. The Schistes Lustrés suite contains units for which peak-metamorphic *P-T* conditions define a trajectory similar to that experienced in modern subduction zones and that were exhumed along isothermal to down-temperature exhumation paths, the latter resulting in minimal retrogradation and preservation of prograde devolatilization history (Agard et al., 2001; Bebout et al., 2013). These rocks are well characterized through detailed field, petrologic, and geochemical studies that considered the degree of evolution in concentrations of volatiles, whole-rock and single-mineral trace element concentrations, and stable isotope compositions of several trace elements thought to be particularly mobile in H_2O-rich metamorphic fluids (Barnes et al., 2019; Bebout et al., 2013; Busigny et al., 2003; Cook-Kollars et al., 2014).

We present Tl concentrations and isotope compositions for a suite of 18 metapelitic samples previously studied by Bebout et al. (2013) and from units together reflecting peak metamorphism over a *P-T* range of 300–550 °C and 1.5–3.0 GPa (also see Barnes et al., 2019). The examination of this suite allows a detailed comparison of the behavior of Tl with that of a number of other fluid-mobile elements of particular interest in considering subduction zone chemical cycling (N, B, Cs, Li, and Cl). We consider the utility and the potential limitations of using Tl geochemistry to interpret subduction zone processes, including a consideration of the effects of post-peak-metamorphic overprinting.

2. Geologic setting

The Schistes Lustrés and Lago di Cignana localities in the western Alps, Italy represent pelagic sedimentary rocks that were subducted under cool end-member subduction conditions, which together reflect peak *P-T* conditions over ranges of 300–550 °C and 1.5–3.0 GPa, in line with those experienced in most modern subduction zones (Fig. 1, see Supplementary material for coordinates of sampling locations) (Agard et al., 2000, 2001; Barnes et al., 2019; Bebout et al., 2013). The metasedimentary rocks of the Schistes Lustrés display changing mineralogy during prograde subduction metamorphism, with quartz, phengite, carbonate, and chlorite present across all grades; however chlorite in the later stages is rare and appears to be retrograde (Agard et al., 2000, 2001; Bebout et al., 2013; Cook-Kollars et al., 2014). The abundance of calc-silicate minerals such as clinozoisite, garnet, titanite, and epidote (among others) greatly increases between the Albergian and Finestre stages of metamorphism (grades C and D) (Cook-Kollars et al., 2014). Other accessory phases, such as rutile, apatite, and oxides, are also present in most samples, although their occurrence generally increases within later metamorphic grades. For a more detailed summary of mineralogical changes and mineral chemistry, please refer to Agard et al. (2001), Bebout et al. (2013), and Cook-Kollars et al. (2014). The shift in mineralogy is accompanied by ~20% dehydration, largely driven by the breakdown of chlorite, and to a lesser extent carpholite and lawsonite, at *P-T* conditions between those represented by the Albergian and Finestre units (Bebout et al., 2013).

Several traditional isotope systems (H, C, N, and O) show little or no variation in isotope compositions with metamorphic grade or devolatilization in the Schistes Lustrés (Bebout et al., 2013; Busigny et al., 2003). Similarly, many traditionally fluid-mobile elements, such as N, B, Li, Cs, Ba, and Rb, were found to be largely immobile; rather than being lost to fluids during devolatilization, these elements were redistributed within evolving mineral assemblages with increasing metamorphic grade (Barnes et al., 2019; Bebout et al., 2013). Interestingly, while Li concentrations displayed no discernible variation across metamorphic grade, there was significant variation in Li isotope composition believed to reflect differential chemical weathering of the protolith (Barnes et al., 2019). These existing studies on the same suite of samples provide an excellent framework with which to interpret the effect of prograde geochemical processes on another traditionally fluid-mobile element, Tl.

Table 2
In situ mineralogical thallium and manganese concentrations via LA-ICP-MS for each metamorphic grade.

Chlorite	MM grade	*Fraiteve – grade A*	*Assietta – grade B*	*Albergian – grade C*	*Finestre – grade D*	*Cignana – grade E*
	WR contribution	13%	ND	*10%*	*13%*	*3%*
	[Tl] (μg/g)	0.46	0.09	*0.04*	*BDL*	*0.02*
	[Mn] (μg/g)	3.4	1.8	*1.6*	*1.5*	*3.7*
Phengite	MM grade	*Fraiteve – grade A*	*Assietta – grade B*	*Albergian – grade C*	*Finestre – grade D*	*Cignana – grade E*
	WR contribution	21%	17%*	59%	36%	36%
	[Tl] (μg/g)	1.3	1.9	2.1	2.2	2.8
	[Mn] (μg/g)	0.20	0.09	0.04	0.30	0.10
	Calculated WR [Tl] (ng/g) from in situ data	330	320	1240	790	1000

Whole rock (WR) contribution is calculated from point counting and denotes the overall fraction of that particular mineral that makes up the rock sample. *denotes an average value from phengite grains and a mixture of quartz/fine-grained phengite identified during point counting. Values for Cignana (grade E) are the average of 3 thin sections that were analyzed; all other grades utilized one representative thin section. Each mineral of interest was analyzed a minimum of five times and averaged. ND denotes mineral constituents that were not detected during point counting. BDL = below detection limit. Italicized chlorite samples for grades 3–5 denote that chlorite here is believed to be retrograde (Cook-Kollars et al., 2014). WR [Tl] is calculated using the WR contribution and mineralogical [Tl] shown here. For comparison, measured WR [Tl] is denoted in Table 1.

3. Methods

3.1. Sample preparation

Powdered samples were digested at the University of Massachusetts Lowell and generally ranged from 20 to 80 mg of material. Samples were first digested with 1 mL of concentrated, distilled HNO_3 plus 3 mL of concentrated HF in high-pressure PTFE bombs within an oven at 160 °C for a minimum of 3 days. Samples were then transferred to 15 mL Savillex screw-top beakers where they were evaporated and then refluxed in 4 mL of distilled aqua regia on a hot plate at 140 °C for a minimum of 24 h to remove any remaining fluorides. Samples were uncapped and evaporated, with the resulting salts repeatedly dissolved in 3 mL of 6N distilled HCl at 140 °C until a solution free of precipitates was obtained. This typically required 2–3 cycles of 6N HCl refluxing. Once any remaining precipitates were removed, the samples were uncapped, evaporated, and brought up in 1 mL of 5% HNO_3. An aliquot of this solution was used for Tl and trace element concentration analysis and the remaining solution underwent Tl separation and isotope analysis at the National High Magnetic Field Laboratory at Florida State University. Additionally, four USGS rock standards (BHVO-2, BIR-1a, BCR-2, and NOD-A-1) were digested to use as external standards for trace element concentration calibration and/or Tl isotope composition measurements. All USGS standards were consistent with reported literature values (Table 1).

3.2. Whole rock thallium concentration measurements

A 50 μL aliquot of each sample and USGS rock standard solution was diluted to 5 mL with 5% HNO_3. Solutions were spiked with 20 ng/g indium as an internal standard to correct for instrumental drift. The USGS rock standards provided an external standard calibration curve for the determination of trace element concentrations. Solutions were analyzed on an Agilent 7900 quadrupole inductively-coupled-plasma mass spectrometer (ICP-MS) within the University of Massachusetts Lowell Core Research Facility. Additionally, Tl concentrations were also calculated based on comparison to solution standards during Tl isotope composition analysis via multi-collector inductively-coupled-plasma mass spectrometer (MC-ICP-MS) (see Section 3.4.) for comparison of analytical uncertainty.

3.3. In situ mineralogical thallium concentration measurements

One representative sample from each metamorphic grade was selected to create a thin section. The final metamorphic grade was the only exception, where three samples were selected for thin section work to ensure any mineralogical variability was captured. These thin sections were utilized for in situ laser ablation analyses. Mineral phases were first identified via petrography and point counting and subsequently analyzed via electron probe microanalyzer (EPMA) housed in the University of Massachusetts Amherst Department of Geosciences Electron Microprobe/SEM Facility. Quantitative analysis was carried out via Cameca SXFive-TACTIS, with optimized LaB6 source, 5 WDS spectrometers, integrated Bruker SDD-EDS, and Cameca's Peaksight control software. All analyses utilized a 15 kV, 20 nA beam, nominally focused for non-beam sensitive phases (garnet, oxides, sulfides) and slightly defocused (2–5 μm diameter) for beam sensitive phases, such as hydrous phases and carbonates. Applicable mineral and oxide standards were calibrated prior to analysis and matrix corrections were implemented via the PAP method (Pouchou and Pichoir, 1984). EPMA data obtained provided internal standardization for laser ablation inductively-coupled-plasma mass spectrometer (LA-ICP-MS) thallium concentration analysis, with Si, Fe, and Ca being used as internal standards for silicates, sulfides and oxides, and carbonates, respectively (see Supplementary material for EPMA data). LA-ICP-MS analyses were conducted with a Teledyne-CETAC LSX-213 G2 Nd:YAG laser coupled to an Agilent 7900 ICP-MS in the Core Research Facility at the University of Massachusetts Lowell (see Supplementary material for laser parameters). A minimum of five LA-ICP-MS measurements were taken on various grains for each mineral of interest within each thin section and then averaged (Table 2). NIST-610 glass was used as a primary external standard while NIST-612 and USGS BHVO-2G were used as secondary standards. NIST-612 and USGS BHVO-2G glasses were both consistent with reported literature values, 14.6 ± 0.9 μg/g and 0.016 ± 0.003 μg/g, respectively (Nielsen and Lee, 2013).

3.4. Whole-rock thallium separation and isotope composition measurements

Thallium column chromatographic separation and isotope analyses were conducted in the National High Magnetic Field Laboratory at Florida State University with Tl isotope analyses being performed on a Neptune MC-ICP-MS with an Aridus II desolvating nebulizer. Purification of Tl was achieved from a two-column procedure described in detail by Baker et al. (2009), Nielsen et al. (2004), and Rehkämper and Halliday (1999). Samples in this study had a high Pb:Tl ratio and therefore required three-column passes for Tl purification, one large-volume column pass followed by two small-volume column passes. Purified Tl separates were spiked with NIST 981 Pb to monitor for internal mass bias. Additionally, this also allowed for the determination of Tl concentrations during isotopic analysis given the yield of the Tl column chemistry is near 100% (Owens et al., 2017; Prytulak et al., 2013). Thallium isotope analyses utilized standard-sample bracketing with a mixed NIST 997-NIST 981 standard solution as well as mass bias

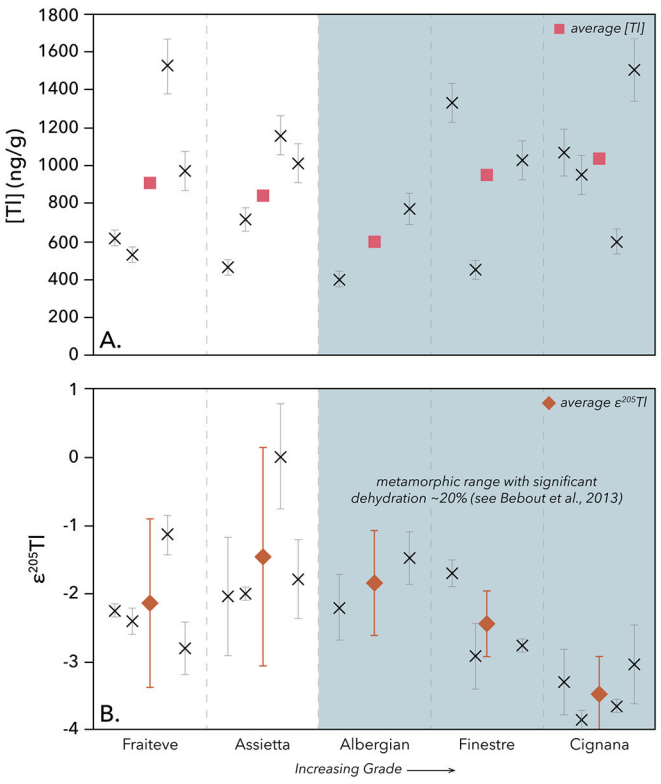

Fig. 2. A.) Whole rock Tl concentration results for each sampling locality within the Schistes Lustrés region, presented in order of increasing metamorphic grade. Individual samples are shown with an X with the error bars representing 2σ, which denotes the instrumental uncertainty of 10%. Average values for each metamorphic range are denoted with a square. Error bars for average values are not included here as 2σ (the standard deviation between all samples averaged) is nearly the entire range of concentrations shown for each metamorphic grade. B.) Whole rock ε^{205}Tl results for each sampling locality within the Schistes Lustrés region, presented in order of increasing metamorphic grade. Individual samples are denoted with an X with the error bars representing 2σ, which denotes the variability between three runs of a single sample. Average values for each metamorphic range are denoted with a diamond with the error bars representing 2σ, the standard deviation between all samples averaged.

correction of the measured ^{205}Tl/^{203}Tl isotope ratios relative to the added NIST 981 Pb. Thallium isotope compositions are reported relative to NIST 997 (ε^{205}Tl = 0). Analyses of USGS reference materials BHVO-2, BCR-2, and NOD-A-1 yielded mean ε^{205}Tl values of −1.43 ± 0.3 (n = 4), −2.2 ± 0.3 (n = 6), and + 11.2 ± 0.3 (n = 3), respectively, which are consistent with reported literature values (Brett et al., 2018; Nielsen et al., 2017b; Prytulak et al., 2013). Blanks were below detection limit for both Tl and Pb. The errors here, and for all reported samples, represent two standard deviations of replicate analyses, with the total number (n) of analyses denoted following each mean ε^{205}Tl value.

4. Results

4.1. Whole-rock thallium concentrations

Thallium concentrations vary slightly as a function of metamorphic grade. The values collected on both the quadrupole ICP-MS and the MC-ICP-MS are in good agreement with each other, generally within 10–15% difference on average (Fig. 2A, Table 1), which is the error on the MC-ICP-MS. Henceforth, unless otherwise noted, any [Tl] referenced within the text or figures will refer to data obtained through MC-ICP-MS methods. Overall, [Tl] ranged from 400 to 1520 ng/g, with [Tl] remaining roughly constant during metamorphism (Fraiteve (unit A): $[Tl]_{avg}$ = 910 ng/g, Assietta (unit B): $[Tl]_{avg}$ = 840 ng/g, Albergian (unit C): $[Tl]_{avg}$ = 590 ng/g, Finestre (unit D): $[Tl]_{avg}$ = 950 ng/g, and Cignana (unit E): $[Tl]_{avg}$ = 1040 ng/g). Overall, there are slight variations in [Tl] across the metamorphic grades, however, these are small and one-way analysis of variance (ANOVA) determined there was no statistically significant difference between them [F(4,12) = 0.474; p = 0.75].

4.2. In situ mineralogical thallium concentrations via LA-ICP-MS

There are distinct mineralogical trends in Tl distribution, with phengite and chlorite being the predominant Tl hosts (Table 2) and only minor Tl associated with minor accessory phases such as rutile, trace sulfides, and minor oxides (these were excluded from Table 2 given their low abundance and [Tl]). During prograde metamorphism, the distribution of phengite present systematically increases, from ~20% of the bulk rock composition (based on point counting) to greater than 30%. This shift toward the larger volumetric abundance of phengite is related to the evolving net volume of the non-phengite portion of the rock and is not a direct increase in the modal abundance of phengite. In other words, there is no new influx of phengite components and, instead, previously stable minerals break down and evolve into new, less volumetric mineral phases (Bebout et al., 2013). This results in an overall increase in phengite volume without the formation of any new phengite material. Chlorite, on the other hand, decreases from ~13% of the bulk rock composition at the lowest metamorphic grade to less than 5% at the highest metamorphic grade. Previous work (Cook-Kollars et al., 2014) indicates chlorite present at the three highest grades of metamorphism is retrograde and would otherwise be unstable under these conditions. Much of the variation in chlorite abundance among these samples is related to bulk compositional differences, with chlorite being more abundant in metapelite samples with lower abundances of carbonates.

Thallium enrichment within these mineralogical components follows the same trend: phengite [Tl] increases during prograde metamorphism, rising from 1.2 ± 1.0 μg/g (avg, n = 5) at the lowest metamorphic grade to 2.8 ± 0.3 μg/g (avg, n = 18, from three thin sections) at the highest metamorphic grade. There was a statistically significant difference of $[Tl]_{pheng,avg}$ between metamorphic grades as determined by ANOVA [F(4,49) = 11.374; p = 1.32E-06]. Post hoc comparisons between treatment types using the Tukey HSD test indicated that the mean values for $[Tl]_{pheng,avg}$ of the two lowest metamorphic grades differed significantly from $[Tl]_{pheng,avg}$ of the highest metamorphic grade at $p < 0.05$. Chlorite [Tl] drops from 0.46 ± 1.0 μg/g (avg, n = 11) to 0.02 ± 0.03 μg/g (avg, n = 10, from two thin sections) from the lowest grade rocks to the highest grade rocks, respectively. Again, previous work indicates that chlorite present in the three highest grades is almost certainly retrograde in origin (Cook-Kollars et al., 2014). There was not a statistically significant difference of $[Tl]_{chl,avg}$ between metamorphic grades as determined by ANOVA [F(3,31) = 2.009; p = 0.13]. Even with the chlorite [Tl] remaining statistically consistent across all metamorphic grades, the contribution of chlorite Tl to the overall Tl budget does decrease, given the overall decrease in the modal abundance of chlorite during prograde metamorphism.

4.3. Thallium isotope compositions

Thallium isotope compositions vary as a function of metamorphic grade (Fig. 2B). Overall, ε^{205}Tl values range from −3.8 (± 0.3) to 0.0 (± 0.8), with ε^{205}Tl values remaining fairly consistent during the first three stages of metamorphism (Fraiteve: (unit A) $\varepsilon^{205}Tl_{avg}$ = −2.1 ± 1.3, Assietta (unit B): $\varepsilon^{205}Tl_{avg}$ = −1.5 ± 1.7, and Albergian (unit C): $\varepsilon^{205}Tl_{avg}$ = −1.9 ± 0.8) and then systematically shifting to more negative values during further stages of metamorphism (Finestre (unit D): $\varepsilon^{205}Tl_{avg}$ = −2.4 ± 1.0, and Cignana (unit E): $\varepsilon^{205}Tl_{avg}$ = −3.5 ± 0.6). There was a statistically significant difference of ε^{205}Tl compositions between metamorphic grades as determined by ANOVA [F(4,12) =

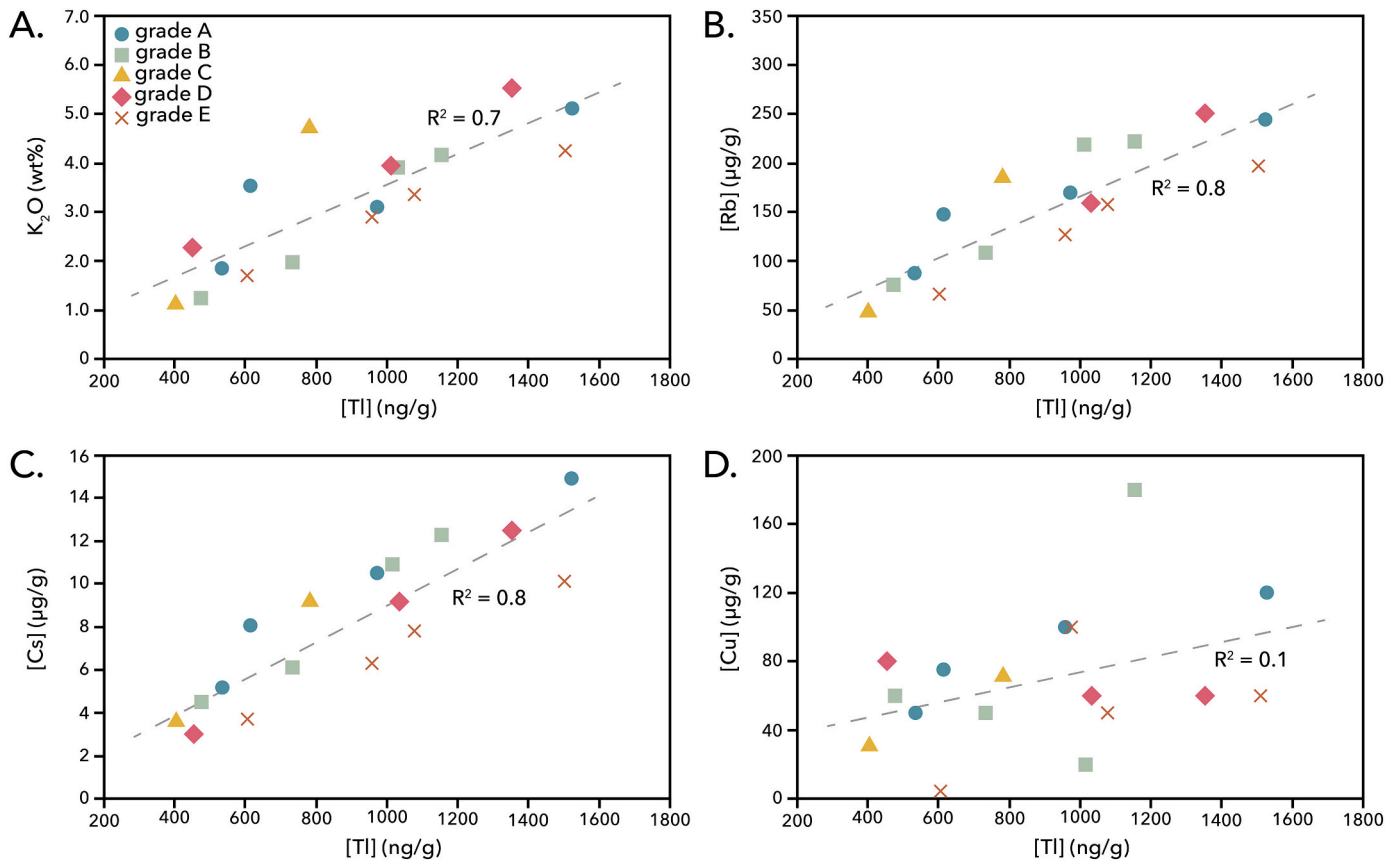

Fig. 3. Whole rock Tl concentration data plotted against (A) K_2O (wt%), (B) Rb (µg/g), (C) Cs (µg/g), and (D) Cu (µg/g) for Schistes Lustrés. Data for K_2O, Rb, Cs, and Cu are from Epstein et al., 2020. Data for Tl are from this study and reference the MC-ICP-MS data. Various colors represent the varying metamorphic grade of samples.

4.639; $p = 0.02$]. Post hoc comparisons between treatment types using the Tukey HSD test indicated that the mean values for ε^{205}Tl for the second metamorphic grade (Assietta) differed significantly from those for the final metamorphic grade (Cignana) at $p < 0.05$. The mean ε^{205}Tl values for the first metamorphic grade (Fraiteve) also differed significantly from those of the final metamorphic grade (Cignana), but at $p < 0.1$ ($p = 0.08$).

5. Discussion

5.1. Thallium concentration systematics

Thallium has previously been shown to be fluid-mobile (Baker et al., 2010; Nielsen et al., 2015; Shaw, 1952); thus, it would be expected that during prograde slab dehydration Tl would be lost to the resulting fluid. However, the results for the Schistes Lustrés display little or no net change (gain or loss) of Tl during systematic, prograde metamorphism, including during slab dehydration at high metamorphic grades (Fig. 2A). Instead, we assert that Tl is concentrated in phengite at higher metamorphic grades, where it can be retained at least to depths approaching those beneath volcanic fronts (as shallow as 70-80 km) (Syracuse and Abers, 2006). This signifies that Tl inherited from the original subduction package is relatively immobile and can largely be passed from slab to arc magmas. However, experimental work on the stability of phengite demonstrates it may be stable well beyond the depths of melt generation, anywhere from 180 to 240 km in warmer subduction zones and up to depths exceeding 360 km in cool, mature subduction zones, such as at Schistes Lustrés (Domanik and Holloway, 1996). Therefore, it is uncertain whether the Tl in the original subduction package is efficiently transferred to arc magmas.

Rather than regional-scale processes affecting Tl mobility, mineralogical variations, namely the presence of sheet silicates such as phengite and to a lesser extent chlorite, may dictate degrees of Tl retention or liberation during subduction metamorphism. This behavior has been found in various HPLT terranes (Shu et al., 2019) and previous studies of arc lavas (Nielsen et al., 2016, 2017b; Prytulak et al., 2013). Rader et al. (2018) demonstrated the near-ubiquity of Tl enrichment in sheet silicates as compared to coexisting framework silicates and sulfides and the influence the presence of K^+ has on the mineralogical Tl enrichment. In the Schistes Lustrés, the same relationship is observed, with whole rock [Tl] positively correlating with whole-rock concentrations of K, Cs, and Rb (Fig. 3) and thus linked to the abundance of phengite (Hermann and Rubatto, 2009; Shu et al., 2019). While there is no overall net loss or gain of Tl during subduction for these samples (Fig. 2A), there is a noted shift in mineralogical abundance, with chlorite no longer stable during the dehydration stages of metamorphism and the modal abundance of phengite remaining constant. A very small increase in the volumetric abundance of phengite with increasing grade, in the calculations by Bebout et al. (2013) and Cook-Kollars et al. (2014), is related to a change in the molar volume of the non-phengite portion of the rock and does not reflect an increase in the abundance of phengite (see Section 5.2.1. for additional discussion of phengite stability). At the higher grades, elements such as Li and Tl become more concentrated in phengite as they are released during chlorite breakdown (for Li, see the discussion in Bebout et al., 2013).

Using the modal abundances gained from point counting along with chlorite and phengite Tl concentrations (see Table 2), whole-rock [Tl] can be reproduced (Table 1), within error (±15%), for the final two grades of metamorphism. However, there is a noted disagreement between the measured whole-rock [Tl] and the mass-balance calculated

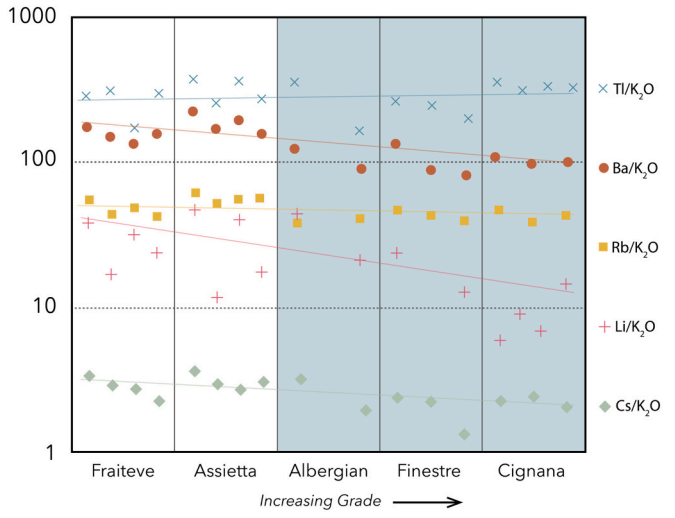

Fig. 4. Assessment of element mobility and crystallographic controls on fluid-mineral partitioning within the Schistes Lustrés. Behavior of selected lithophile elements with increasing metamorphic grade show loss of Ba, Cs, and Li compared to K_2O and no loss of Tl or Rb. The lines for each dataset are lines of best fit to demonstrate behavior overall. Thallium data are from this study (see Table 1) while other elemental data are from Epstein et al., 2020. Blue coloration for later stages of metamorphism denotes significant (~20%) dehydration of the slab (see Bebout et al., 2013). No loss compared to K_2O signifies a strong phengite control on elemental immobility, as shown for Tl and Rb. Elements that decrease with increasing grade, and particularly during dehydration, such as Ba, Li, and Cs, likely have another mineralogical reservoir.

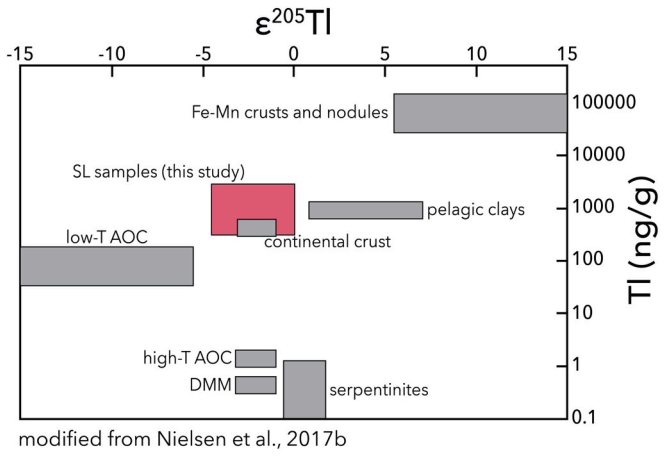

Fig. 5. Thallium concentration and isotope compositions for common terrestrial reservoirs. Data from the Schistes Lustrés region (SL) are included here in pink for comparison. Schistes Lustrés isotopic data trend to lower values with increasing metamorphic grade. AOC = altered oceanic crust. DMM = depleted MORB mantle. Original figure modified from Nielsen et al., 2017b. Serpentinite data from Nielsen et al., 2015.

whole-rock [Tl] from phengite and chlorite modal abundances for the first three stages of metamorphism. At lower grades of metamorphism, there may be additional, minor mineralogical hosts of Tl that nevertheless impact the whole rock Tl abundance, such as minor sulfides, other sheet silicates like stilpnomelane, or minor oxides, that should be further characterized for variations in [Tl] as well as ε^{205}Tl compositions. Indeed, sulfides, oxides, carbonates, and other sheet silicates are present at lower grades. However, they were either not captured during point counting or had such a low overall abundance (as determined by point counting) and/or [Tl] (as determined by LA-ICP-MS) that they did not contribute significantly during our calculations. This disagreement between calculated and measured WR [Tl] at lower grades of metamorphism highlights the need for further studies which can attempt to measure mineralogical variations more accurately, including Tl isotopic compositions. Some of the overall Tl variability within each grade likely reflects compositional differences as individual samples from each metamorphic unit contain varying levels of Tl-bearing minerals, such as phengite and chlorite. This gives a more accurate overview of the metamorphic unit as a whole, but may result in larger disagreement between individual samples.

Overall, progressive breakdown of chlorite during subduction likely released Tl that was then incorporated into newly recrystallized phengite during more progressive stages of metamorphism, as noted by the consistent behavior of Tl when normalized to K_2O across all metamorphic grades (Fig. 4) (Barnes et al., 2019; Bebout et al., 2013; Penniston-Dorland et al., 2012). Ratios of the "fluid-mobile" elements such as Ba, Cs, Li, and Tl to the concentrations of K_2O serve to normalize chemical heterogeneities among whole rock samples, particularly with respect to phengite as it is the dominant K-phase. Concentrations of Ba, Cs, and Li show a slight decrease during progressive metamorphism (see the normalization to K_2O in Fig. 4). In addition to possible loss to fluids, this could arise from the fact that these elements have additional potential hosts at both low and high metamorphic grades allowing for greater mineralogical variation during prograde metamorphism. For example, at lower grades, Li may be able to substitute both within the 8-fold coordination environment of the Mg—Fe carpholite structure and the 6-coordinated position of Fe and Mg within the chlorite structure ($^{VIII}Fe^{2+}$ = 0.92 Å, $^{VIII}Mg^{2+}$ = 0.89 Å, $^{VIII}Li^{+}$ = 0.92 Å; $^{VI}Fe^{2+}$ = 0.61 Å, $^{VI}Mg^{2+}$ = 0.72 Å, $^{VI}Li^{+}$ = 0.76 Å) and ultimately be transferred into the dehydrating fluid (Shannon, 1976). At higher metamorphic grades, paragonite may be a potential additional host for Ba, whereas the smaller 6-coordinated position of Na within paragonite is not suitable for Tl substitution ($^{VI}Na^{+}$ = 1.02 Å, $^{VI}Ba^{2+}$ = 1.35 Å, $^{VI}Tl^{+}$ = 1.50 Å) (Shannon, 1976).

Although previous studies have found that sulfides may be a dominant Tl host during mantle melting (Coggon et al., 2014; Kiseeva and Wood, 2013; Nielsen et al., 2014), there is no correlation observed here between Tl and Cu (Fig. 3) or Tl and Fe (not shown), indicating sulfides are unlikely to be a significant contributor to the overall Tl budget in this subduction terrane. This is in agreement with previous mineralogical work (Rader et al., 2018) and more general results from subducted oceanic crust (Shu et al., 2019) and points to phengite being the predominant mineralogical host for Tl in the Schistes Lustrés.

5.2. Causes for distinct shifts in thallium isotope compositions

The consistency of [Tl] coupled with the varying ε^{205}Tl compositions during prograde metamorphism suggest a predominantly internal mechanism responsible for Tl isotope fractionation, particularly during dehydration throughout higher grades of metamorphism. During the final three stages of metamorphism, the ε^{205}Tl compositions in the Schistes Lustrés are progressively shifted to lower values (Fig. 2B). Recent studies have revealed that small additions of Mn-rich pelagic clays or AOC may significantly affect the Tl budget of arc materials (Nielsen et al., 2016, 2017b; Prytulak et al., 2013); however, both of these processes would result in more significant [Tl] variation or more extreme fluctuations in ε^{205}Tl compositions than observed here (Fig. 5).

Pelagic sediments that have been shown to cause significant variations in the Tl budget of arc materials are Mn-rich (Nielsen et al., 2017b). The strong enrichment of Mn in pelagic clays causes local oxidation of Tl^{+} to Tl^{+3}, resulting in significantly higher ε^{205}Tl compositions, with $\varepsilon^{205}Tl_{avg}$ = +3 to +5 (Prytulak et al., 2013; Rehkämper et al., 2004). Therefore, any addition of Mn-rich pelagic sediments would shift ε^{205}Tl compositions to more positive values, not negative values as observed in the Schistes Lustrés. Additionally, the rocks in the Schistes Lustrés are generally Mn-poor (Table 1).

The shift to more negative ε^{205}Tl values during devolatilization may

result from buffering of Tl by fluids released from underlying AOC. Minor Tl could be lost from the slab with increasing metamorphic grade, but the loss of Tl from the slab could be roughly matched with an equivalent addition of Tl from the fluid flux of the underlying oceanic crust. This could result in a relatively consistent [Tl] across metamorphic grades, but a noted change in ε^{205}Tl, if the underlying oceanic crust had a significantly different ε^{205}Tl signature compared with the subducting pelitic material. According to mass balance and an average ε^{205}Tl = −7.2 and [Tl] = 100 ng/g for AOC (Nielsen et al., 2017b), the total incorporation of ~27% of AOC-derived Tl would be required to account for the shift in ε^{205}Tl compositions observed here between the first and final stages of metamorphism. However, this large volume of AOC required would also result in a significant overall decrease in [Tl], on the order of several hundred ng/g lower than the observed values in the Schistes Lustrés, given that AOC Tl concentrations are nearly an order of magnitude lower than what we observe here (Figs. 2 and 5) (Nielsen et al., 2017b; Shu et al., 2017). This suggests that fluid buffering from AOC is unlikely to be responsible for the observed Tl systematics here. Additionally, it is expected that fluids released from AOC would result in a high Ba/Th ratio in phengite-bearing metamorphic rocks and a lower Ce/Tl ratio that correlates to lower isotopic compositions as more AOC-derived fluid is added. However, we do not observe these trends, with Ba/Th ratios being more than an order of magnitude lower than expected (Shu et al., 2019) and there being no correlation between Ce/Tl ratios and ε^{205}Tl values at Schistes Lustrés.

Rather than AOC acting as the buffer, similar to B in the Lago di Cignana complex (Halama et al., 2020), it is possible the variation in ε^{205}Tl during later stages of metamorphism is a result of fluid-rock interaction from an influx of overprinting serpentinite-derived fluid. However, this is also unlikely as serpentinite samples from the Mariana forearc all display much higher ε^{205}Tl values, with ε^{205}Tl > −0.5 (Nielsen et al., 2015). Any incorporation of such a fluid would result in a shift toward more positive ε^{205}Tl compositions, not negative ε^{205}Tl compositions as observed here, and a significant decrease in the whole rock [Tl] (Fig. 5). Furthermore, there is no statistical variation of [Tl] or any correlation between [Tl] and ε^{205}Tl as is observed for B and modeled via retrograde fluid-rock equilibration. Buffering of the slab from an externally-derived or metamorphic fluid should not be entirely ruled out. But, for buffering of this sort to have occurred, a fluid of similar Tl enrichment but with notably lower Tl isotopic composition is required, which has not been identified as yet.

Given their similar geochemical behavior in the Schistes Lustrés, the Tl isotopic composition may have the same controlling mechanism as that of Li isotopes. In the Schistes Lustrés, Li concentrations remain fairly consistent across metamorphic grades, but with a noted shift in Li isotopic compositions (Barnes et al., 2019). This was initially inferred to be the result of fluid-mineral partitioning, however it was anticipated that if fluid-mineral partitioning was responsible for the observed isotopic effects of Li, it would behave similarly to Tl, with the heavier Li isotope preferentially moving into the fluid phase, leaving the resulting rocks with much lower Li isotopic compositions after dehydration. The behavior of Li isotopes in relation to metamorphic grade is the opposite of that predicted. Rather than becoming more negative with increasing grade, Li isotope compositions become increasingly more positive with increasing grade (Barnes et al., 2019). Given this conflicting behavior, the observed fractionation in Li isotopes was inferred to be a result of differential weathering of the protolith, or the chemical index of alteration (CIA). This means that the Li isotopic composition of the original sediment inherited from surface weathering remains intact throughout subduction. However, the correlation between CIA and ε^{205}Tl compositions is not statistically significant at the 95% confidence interval (p = 0.1), making this association more difficult to infer or confirm for the Tl system (see Supplementary material). Nevertheless, some of the variability observed here may be an indicator of original protlith composition variability, without the influence of surface weathering.

There is a noted degree of isotopic variability within each metamorphic unit, particularly at lower grades, which may reflect sample composition heterogeneity and may also explain the mismatch between calculated and measured whole rock [Tl]. Given that the Tl systematics of this region seem to be controlled by such a small number of mineralogical hosts, primarily phengite and chlorite, then it would be expected that inherited compositional variability influencing whole rock Tl isotopic compositions would also be prevalent within the Tl concentration values for each grade. While there is overall [Tl] variability within grades, the consistency and lack of any statistically significant changes in average Tl concentrations across grades (see Section 4.1.) seems to preclude this behavior. Additional, mineral-specific work is required to better quantify any effect inherited protolith heterogeneity may have on whole rock Tl values.

5.2.1. *Fluid-mineral Tl isotopic fractionation*

The small, but resolvable and significant negative shift in ε^{205}Tl compositions during prograde metamorphism in the Schistes Lustrés may be controlled by fluid-mineral partitioning induced by mineralogical variations coupled with fluid fluxing during slab dehydration. The observed shift in ε^{205}Tl values corresponds with significant dehydration, on the order of ~20% total fluid loss, during prograde metamorphism in the approximate temperature range of 450–550 °C (Bebout et al., 2013; Cook-Kollars et al., 2014). This fluid fluxing is primarily attributed to the breakdown of chlorite (and to a lesser extent carpholite and lawsonite) at high T (Bebout et al., 2013; Cook-Kollars et al., 2014). The minor amount of chlorite that is present in later stages of metamorphism (grades 3–5) appears to be retrograde (Cook-Kollars et al., 2014), thus not reflective of original, equilibrium conditions.

Simultaneous to the chlorite breakdown, the net modal proportion of phengite systematically increases; however, this increase is not accompanied by an increase in either K_2O or [Tl] (Table 1). These consistencies indicate the fluxing of the devolatilization fluid was not a contributing mechanism in supplying additional material for the formation of phengite, as was observed for subducted low-T AOC at Tien Shan (Shu et al., 2019). Instead, Tl was redistributed among recrystallized phengite that was evolving in major and trace element compositions as prior Tl hosts, such as chlorite and other mineral constituents became unstable. This redistribution of trace elements among shifting mineralogy during subduction dehydration may have led to a small, but discernible, equilibrium isotopic fractionation of Tl between the recrystallized mineralogical phases and the fluid, assuming a minor amount of chlorite-borne Tl was lost to the fluxing metamorphic fluid. There are likely additional, minor Tl hosts that may have also lost a small amount of Tl to the fluid phase, particularly considering that whole-rock [Tl] cannot be reproduced from phengite and chlorite mineralogical data for the first three grades of metamorphism (see Section 5.1.).

The degree of isotopic fractionation would then become a function of coordination number, with the lower coordination number leading to a preference for the heavier Tl isotope (^{205}Tl). Within the chlorite structure, Tl is presumed to substitute in the 6-coordinated position of Fe, Mg, and/or Mn ($^{VI}Tl^{+}$ = 1.50 Å, $^{VI}Fe^{2+}$ = 0.61 Å, $^{VI}Mg^{2+}$ = 0.72 Å, $^{VI}Mn^{2+}$ = 0.67 Å), while within phengite, Tl is presumed to substitute in the much larger, 12-coordinated K site within the interlayer structure ($^{XII}Tl^{+}$ = 1.70 Å, $^{XII}K^{+}$ = 1.64 Å) (Shannon, 1976). Of note, there is significant Mn present within the chlorite at lower grades in the Schistes Lustrés, which could result in a non-insignificant accumulation of the heavier Tl isotope given the distinct effect of Mn on shifting Tl isotope compositions to more positive values (Fig. 2B): Mn-rich sediments have recorded the heaviest Tl isotopic compositions currently measured, given the ability of Mn-oxides to adsorb and oxidize Tl at their surface (Nielsen and Lee, 2013; Nielsen et al., 2017a, 2017b; Peacock and Moon, 2012). This results in the sorbed Tl becoming enriched in ^{205}Tl and induces isotopic fractionation, resulting in more positive ε^{205}Tl values. Mn-rich sheet silicates have been shown to demonstrate similar behavior, with Mn-bearing muscovite having significantly higher ε^{205}Tl values than other sheet silicates (Rader et al., 2018). This heavier signature would

presumably be lost to the fluid phase during slab dehydration given the similar bonding environments between Tl in chlorite and the solution: Tl is assumed to be in 6-fold coordination in fluids, although there is limited experimental or other evidence to support this claim (Lincoln et al., 2003). Thus, ^{205}Tl should preferentially partition into aqueous fluids relative to phengite, resulting in more positive ε^{205}Tl values for the fluid, causing more negative ε^{205}Tl values remaining in the phengite-bearing rocks. If we assume 20% fluid loss during dehydration (Bebout et al., 2013), that the Tl isotopic composition of the final metamorphic stage is representative of the remaining 80% of the Tl reservoir ($\varepsilon^{205}Tl_{Cignana} = -3.5$), and utilize a mass balance equation, we can estimate the composition of the fluid lost, $\varepsilon^{205}Tl_{fluid}$. With an overall decrease of 1.4 ε^{205}Tl for the whole rock samples (from $\varepsilon^{205}Tl_{Fraiteve} = -2.1$ to $\varepsilon^{205}Tl_{Cignana} = -3.5$), our calculated $\varepsilon^{205}Tl_{fluid} = +3.5$. With $\varepsilon^{205}Tl_{fluid} = +3.5$ and $\varepsilon^{205}Tl_{Cignana} = -3.5$, we can then calculate the fractionation factor between the two, where $\alpha_{fluid/rock} = \frac{\varepsilon^{205}Tl_{fluid}+10{,}000}{\varepsilon^{205}Tl_{rock}+10{,}000}$. This results in a positive Tl fluid with a fractionation factor of $\alpha_{fluid/rock} = 1.0007$. Using this information, we can model this fluid-mineral partitioning process via Rayleigh distillation. In doing so, ~10% of the total Tl being lost to the fluid results in the $\varepsilon^{205}Tl_{rock}$ values observed here between grade A and grade E, which would also maintain a [Tl] within analytical uncertainty of the values measured in the Schistes Lustrés (Table 1). While this modeling approach isn't ideal, given the limited data available on fluid mineral partitioning at P and T constraints applicable here for the Schistes Lustrés for comparison, this indicates as a first-pass approximation that dehydration-induced mineral destabilization and growth during subduction metamorphism may be able to alter bulk rock ε^{205}Tl compositions without significantly affecting the bulk rock [Tl]; the extent of partitioning some Tl to a fluid phase may not be enough to significantly affect the overall [Tl] signature but may result in a noticeable isotopic effect, as observed here.

These findings seem to be at odds with recently published work from subducted oceanic crust from five distinct localities (Shu et al., 2019), which found [Tl] and Tl isotope compositions decoupled, with the implication that phengite did not lead to a fractionation of Tl isotopes. However, there are several distinct differences between those localities and Schistes Lustrés, namely protolith composition, systematics of metamorphism, and overprinting processes. Shu et al. (2019) focused on metabasites as opposed to metapelites in the Schistes Lustrés, which would inherently lead to differences in protolith between the two studies. Furthermore, many of the systems from Shu et al. (2019) also experienced additional coeval or subsequent processes such as low T alteration prior to subduction at Tian Shan, mechanical mixing resulting in blocks within mélange material at Syros, and metamorphic fluid infiltration at Zambia, which may have overprinted or influenced initial Tl compositions. Samples from Schistes Lustrés indicate subduction zone devolatilization was the only process in effect during subduction and exhumation. Schistes Lustrés samples effectively provide a snapshot of Tl behavior at multiple stages along the same subduction path, which allows for tracking changes in Tl imposed by cool end-member subduction zone conditions in a relatively straightforward manner. As such, rather than being at odds with one another, the data presented here and those from Shu et al. (2019) are instead complementary, reflecting Tl behavior in a variety of metamorphic subduction settings for the first time. This indicates the diversity of Tl behavior depending on individual subduction zone mechanisms suggesting heterogeneous response in various subduction zone settings.

6. Conclusions

Thallium appears to be relatively immobile in the Schistes Lustrés and can be retained to depths approaching those beneath volcanic fronts, possibly beyond, during subduction processes. Therefore, Tl should be largely available for introduction into the subarc mantle wedge, at least in environments without any additional complicating factors. The availability of Tl is primarily controlled by sheet silicate phases, namely phengite and to a lesser extent chlorite, as has been predicted for other types of subduction zones (Nielsen et al., 2017b; Shu et al., 2019).

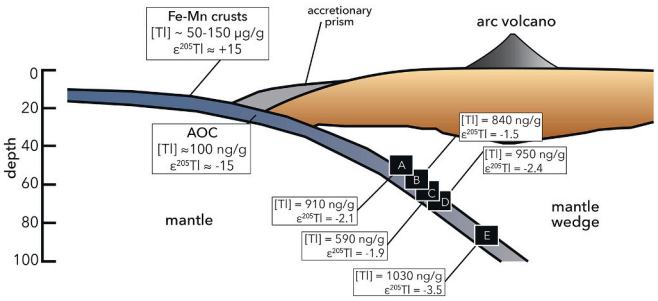

Fig. 6. Schematic showing a generic subduction zone cross section with associated Tl concentration and isotopic composition values at estimated depths comparable to Schistes Lustrés samples (modified from Barnes et al., 2019). The Tl concentration and isotopic composition data at a given depth are based on the average concentration and isotopic composition values of the samples from that specific grade (see Table 1). Significant slab dehydration (~20%) occurs between grades C and D and continues into grade E (see Bebout et al., 2013), which is concurrent with shifts to lower ε^{205}Tl values. Grades are as follows: A = Fraiteve; B = Assietta; C = Albergian; D = Finestre; E = Lago di Cignana. Two prevalent Tl reservoirs are also shown here: Fe—Mn crusts from pelagic sediments and low-temperature altered oceanic crust (AOC) with their accompanying Tl concentration and isotopic data for reference (see Nielsen et al., 2017a, 2017b; Shu et al., 2019).

While simple processes such as forearc devolatilization do not appear to affect Tl concentrations during prograde metamorphism, elemental redistribution induced by mineral destabilization and the formation of a fluid phase during dehydration does appear to alter Tl isotope compositions for higher metamorphic grades (Fig. 6). During dehydration, there may be a small degree of fractionation between mineral and fluid as chlorite and other, minor Tl-bearing mineral components are destabilized and new phengite recrystallizes and evolves in its major and trace element compositions. The fluid fractionation incurred from this process could significantly impact the bulk rock Tl isotopic composition to the point that arc lavas may reflect variations in environment, protolith, or process as opposed to the initial composition of the subducting material. It should be noted that an influx and buffering of an external, metamorphic fluid cannot be entirely ruled out as the mechanism for Tl isotopic fractionation in the Schistes Lustrés, however, a fluid of the required composition has not been identified heretofore. As such, it is important to constrain the systematic controls on Tl behavior at a range of scales related to subduction metamorphism to better understand the utility of using such a system for large scale recycling of Earth's crust.

Declaration of Competing Interest

The authors declare that they have no known competing financial interests or personal relationships that could have appeared to influence the work reported in this paper.

Acknowledgements

Funding for this research was provided by the National Science Foundation grant EAR-1949655 (STR and RMG). JDO acknowledges funding from NASA Exobiology Program, SLOAN Fellowship, and

support for the National High Magnetic Field Laboratory (Tallahassee, Florida), which is funded by the National Science Foundation Cooperative Agreement No. DMR1644779. We thank Dr. Earl Ada for his work maintaining the Core Research Facility at the University of Massachusetts Lowell. We also thank one anonymous reviewer and Dr. Mathias Schannor, as well as the Editor-in-Chief Dr. Catherine Chauvel, for their helpful feedback during revisions of this manuscript. Their reviews made this a much stronger contribution and for that we are grateful.

Appendix A. Supplementary data

Supplementary data to this article can be found online at https://doi.org/10.1016/j.chemgeo.2021.120349.

References

Agard, P., Goffé, B., Touret, J.L.R., Vidal, O., 2000. Retrograde mineral and fluid evolution in high-pressure metapelites (Schistes lustrés unit, Western Alps). Contrib. Mineral. Petrol. 140, 296–315.
Agard, P., Jolivet, L., Goffé, B., 2001. Tectonometamorphic evolution of the Schistes Lustrés complex: implications for the exhumation of HP and UHP rocks in the western Alps. Bull. Soc. Géol. Fr. 172, 617–636.
Andersen, M.B., Elliott, T., Freymuth, H., Sims, K.W.W., Niu, Y., Kelley, K.A., 2015. The terrestrial uranium isotope cycle. Nature 517, 356–359.
Angiboust, S., Agard, P., Jolivet, L., Beyssac, O., 2009. The Zermatt-Saas ophiolite: The largest (60 km wide) and deepest (c. 70–80 km) continuous slice of oceanic lithosphere detached from a subduction zone:? Terra Nova 21, 171–180.
Baker, R.G.A., Rehkämper, M., Hinkley, T.K., Nielsen, S.G., Toutain, J.P., 2009. Investigation of thallium fluxes from subaerial volcanism—implications for the present and past mass balance of thallium in the oceans. Geochim. Cosmochim. Acta 73, 6340–6359.
Baker, R.G.A., Rehkämper, M., Ihlenfeld, C., Oates, C.J., Coggon, R., 2010. Thallium isotope variations in an ore-bearing continental igneous setting: collahuasi Formation, northern Chile. Geochim. Cosmochim. Acta 74, 4405–4416.
Barnes, J.D., Penniston-Dorland, S.C., Bebout, G.E., Hoover, W., Beaudoin, G.M., Agard, P., 2019. Chlorine and lithium behavior in metasedimentary rocks during prograde metamorphism: a comparative study of exhumed subduction complexes (Catalina Schist and Schistes Lustrés). Lithos 336–337, 40–53.
Bebout, G.E., Agard, P., Kobayashi, K., Moriguti, T., Nakamura, E., 2013. Devolatilization history and trace element mobility in deeply subducted sedimentary rocks : evidence from Western Alps HP / UHP suites. Chem. Geol. 342, 1–20.
Blusztajn, J., Nielsen, S.G., Marschall, H.R., Shu, Y., Ostrander, C.M., Hanyu, T., 2018. Thallium isotope systematics in volcanic rocks from St. Helena – constraints on the origin of the HIMU reservoir. Chem. Geol. 476, 292–301.
Brett, A., Prytulak, J., Hammond, S.J., Rehkämper, M., 2018. Thallium mass fraction and stable isotope ratios of sixteen geological reference materials. Geostand. Geoanal. Res. 1–22.
Busigny, V., Cartigny, P., Philippot, P., Ader, M., Javoy, M., 2003. Massive recycling of nitrogen and other fluid-mobile elements (K, Rb, Cs, H) in a cold slab environment: evidence from HP to UHP oceanic metasediments of the Schistes Lustrés nappe (western Alps, Europe). Earth Planet. Sci. Lett. 215, 27–42.
Coggon, R.M., Rehkämper, M., Atteck, C., Teagle, D.A.H., Alt, J.C., Cooper, M.J., 2014. Controls on thallium uptake during hydrothermal alteration of the upper ocean crust. Geochim. Cosmochim. Acta 144, 25–42.
Cook-Kollars, J., Bebout, G.E., Collins, N.C., Angiboust, S., Agard, P., 2014. Subduction zone metamorphic pathway for deep carbon cycling: I . evidence from HP / UHP metasedimentary rocks, Italian Alps. Chem. Geol. 386, 31–48.
Domanik, K.J., Holloway, J.R., 1996. The stability and composition of phengitic muscovite and associated phases from 5.5 to 11 GPa: Implications for deeply subducted sediments. Geochim. Cosmochim. Acta 60, 4133–4150.
Epstein, G.S., Bebout, G.E., Angiboust, S., Agard, P., 2020. Scales of fluid-rock interaction and carbon mobility in the deeply underplated and *HP*-Metamorphosed Schistes Lustrés, Western Alps. Lithos 354-355, 1–18.
Freymuth, H., Vils, F., Willbold, M., Taylor, R.N., Elliott, T., 2015. Molybdenum mobility and isotopic fractionation during subduction at the Mariana arc. Earth Planet. Sci. Lett. 432, 176–186.
Gaschnig, R.M., Reinhard, C.T., Planavsky, N.J., Wang, X., Asael, D., Chauvel, C., 2017. The molybdenum isotope system as a tracer of slab input in subduction zones: an example from Martinique, Lesser Antilles Arc. Geochem. Geophys. Geosyst. 18, 4674–4689.
Halama, R., Konrad-Schmolke, M., De Hoog, J.C.M., 2020. Boron isotope record of peak metamorphic ultrahigh-pressure and retrograde fluid–rock interaction in white mica (Lago di Cignana, Western Alps). Contrib. Mineral. Petrol. 175, 1–19.
Hermann, J., Rubatto, D., 2009. Accessory phase control on the trace element signature of sediment melts in subduction zones. Chem. Geol. 265, 512–526.
Kiseeva, E.S., Wood, B.J., 2013. A simple model for chalcophile element partitioning between sulphide and silicate liquids with geochemical applications. Earth Planet. Sci. Lett. 383, 68–81.
König, S., Wille, M., Voegelin, A., Schoenberg, R., 2016. Molybdenum isotope systematics in subduction zones. Earth Planet. Sci. Lett. 447, 95–102.
Korenaga, J., 2018. Crustal evolution and mantle dynamics through Earth history. Philos. Trans. R. Soc. A376, 20170408.
Lincoln, S.F., Richens, D.T., Sykes, A.G., 2003. Metal aqua ions. In: Comprehensive Coordination Chemistry II. Elsevier, pp. 515–555.
Nielsen, S.G., Lee, C.-T.A., 2013. Determination of thallium in the USGS glass reference materials BIR-1G, BHVO-2G, and BCR-2G and application to quantitative Tl concentrations by LA-ICP-MS. Geostand. Geoanal. Res. 37, 337–343.
Nielsen, S.G., Rehkämper, M., Baker, J., Halliday, A.N., 2004. The precise and accurate determination of thallium isotope compositions and concentrations for water samples by MC-ICPMS. Chem. Geol. 204, 109–124.
Nielsen, S.G., Rehkämper, M., Norman, M.D., Halliday, A.N., Harrison, D., 2006. Thallium isotopic evidence for ferromanganese sediments in the mantle source of Hawaiian basalts. Nature 439, 314–317.
Nielsen, S.G., Shimizu, N., Lee, C.-T.A., Behn, M.D., 2014. Chalcophile behavior of thallium during MORB melting and implications for the sulfur content of the mantle. Geochem. Geophys. Geosyst. 15, 4905–4919.
Nielsen, S.G., Klein, F., Kading, T., Blusztajn, J., Wickham, K., 2015. Thallium as a tracer of fluid–rock interaction in the shallow Mariana forearc. Earth Planet. Sci. Lett. 430, 416–426.
Nielsen, S.G., Yogodzinski, G., Prytulak, J., Plank, T., Kay, S.M., Kay, R.W., Blusztajn, J., Owens, J.D., Auro, M., Kading, T., 2016. Tracking along-arc sediment inputs to the Aleutian arc using thallium isotopes. Geochim. Cosmochim. Acta 181, 217–237.
Nielsen, S.G., Prytulak, J., Blusztajn, J., Shu, Y., Auro, M., Regelous, M., Walker, J., 2017a. Thallium isotopes as tracers of recycled materials in subduction zones: Review and new data for lavas from Tonga-Kermadec and Central America. J. Volcanol. Geotherm. Res. 339, 23–40.
Nielsen, S.G., Rehkämper, M., Prytulak, J., 2017b. Investigation and application of thallium isotope fractionation. Rev. Mineral. Geochem. 82, 759–798.
Owens, J.D., Nielsen, S.G., Horner, T.J., Ostrander, C.M., Peterson, L.C., 2017. Thallium-isotopic compositions of euxinic sediments as a proxy for global manganese-oxide burial. Geochim. Cosmochim. Acta 213, 291–307.
Peacock, C.L., Moon, E.M., 2012. Oxidative scavenging of thallium by birnessite: Explanation for thallium enrichment and stable isotope fractionation in marine ferromanganese precipitates. Geochim. Cosmochim. Acta 84, 297–313.
Penniston-Dorland, S.C., Walker, R.J., Pitcher, L., Sorensen, S.S., 2012. Mantle-crust interactions in a paleosubduction zone: evidence from highly siderophile element systematics of eclogite and related rocks. Earth Planet. Sci. Lett. 319–320, 295–306.
Pouchou, J.-L., Pichoir, F., 1984. A new model for quantitative X-ray microanalysis. La Rech. Aerosp. 3, 167–192.
Prigent, C., Guillot, S., Agard, P., Lemarchand, D., Soret, M., Ulrich, M., 2018. Transfer of subduction fluids into the deforming mantle wedge during nascent subduction: evidence from trace elements and boron isotopes (Semail ophiolite, Oman). Earth Planet. Sci. Lett. 484, 213–228.
Prytulak, J., Nielsen, S.G., Plank, T., Barker, M., Elliott, T., 2013. Assessing the utility of thallium and thallium isotopes for tracing subduction zone inputs to the Mariana arc. Chem. Geol. 345, 139–149.
Rader, S.T., Mazdab, F.K., Barton, M.D., 2018. Mineralogical thallium geochemistry and isotope variations from igneous, metamorphic, and metasomatic systems. Geochim. Cosmochim. Acta 243, 42–65.
Rehkämper, M., Halliday, A., 1999. The precise measurement of Tl isotopic compositions by MC-ICPMS: application to the analysis of geological materials and meteorites. Geochim. Cosmochim. Acta 63, 935–944.
Rehkämper, M., Frank, M., Hein, J.R., Halliday, A., 2004. Cenozoic marine geochemistry of thallium deduced from isotopic studies of ferromanganese crusts and pelagic sediments. Earth Planet. Sci. Lett. 219, 77–91.
Shannon, R.D., 1976. Revised effective ionic radii and systematic studies of interatomic distances in halides and chalcogenides. Acta Crystallogr. A32, 751–767.
Shaw, D.M., 1952. The geochemistry of thallium. Geochim. Cosmochim. Acta 2, 118–154.
Shu, Y., Nielsen, S.G., Zeng, Z., Shinjo, R., Blusztajn, J., Wang, X., Chen, S., 2017. Tracing subducted sediment inputs to the Ryukyu arc - Okinawa Trough system: Evidence from thallium isotopes. Geochim. Cosmochim. Acta 217, 462–491.
Shu, Y., Nielsen, S.G., Marschall, H.R., John, T., Blusztajn, J., Auro, M., 2019. Closing the loop: Subducted eclogites match thallium isotope compositions of ocean island basalts. Geochim. Cosmochim. Acta 250, 130–148.
Spandler, C., Pirard, C., 2013. Element recycling from subducting slab to arc crust: a review. Lithos 170–171, 208–223.
Syracuse, E.M., Abers, G.A., 2006. Global compilation of variations in slab depth beneath arc volcanoes and implications. Geochem. Geophys. Geosyst. 7, 1–18.
Taylor, S.R., 1977. Island Arcs, Deep Sea Trenches and Back-arc Basins. AGU, Washington, DC, pp. 325–335.